Cooperative Manipulation on the Water Using a Swarm of Autonomous Tugboats

Joel Esposito and Matthew Feemster

U.S. Naval Academy
Systems Engineering Department
Annapolis, MD 21402
Email: esposito, feemster@usna.edu

Erik Smith

University of Pennsylvania
Philadelphia, PA
Email: eriksmith_89@hotmail.com

Abstract— In this paper we present a strategy that allows a swarm of autonomous tugboats to cooperatively move a large object on the water. The two main challenges are: (1) the actuators are unidirectional and experience saturation; (2) the hydrodynamics of the system are difficult to characterize. The primary theoretical contribution of the paper addresses the first challenge. We present a tracking controller and force allocation strategy that, despite actuator limitations, result in asymptotically convergent tracking for a certain class of reference trajectories. The primary practical contribution is the introduction of a set of adaptive control laws that address the second challenge by compensating for unknown, and difficult to measure, hydrodynamic parameters. Experimental verification of the controllers is presented using a 1:36 scale model of a U.S. Navy ship, inside the Naval Academy's unique 380 ft testing tank.

I. Introduction

ROBOT swarms are large groups of small, relatively unsophisticated, robots working in concert to achieve objectives that are beyond the capability of a single robot. One example of an application that can benefit from this approach is non-prehensile cooperative manipulation, where a group of non-articulated mobile robots attempts to transport a larger object in the plane, by applying forces to its perimeter. The advantages of the swarm are: (1) its ability to distribute applied forces over a large area, achieving an enveloping grasp on large objects; and (2) the maximum wrench the swarm can exert increases linearly as the number of swarm members increases. We are particularly interested in marine applications involving autonomous tugboats such as towing disabled ships (ex. U.S.S. Cole), transporting components of large offshore structures (ex. oil platforms), or positioning littoral protection equipment (ex. hydrophone arrays). However, most of our group's work can be extended to ground robots as well.

Swarm control strategies represent a very active area of research (see for example [14], [25], [7], [4] and references within). However, most of those works only consider kinematic objectives (i.e., position and velocity), such as collective motion (flocking) or mapping tasks. In cooperative manipulation, second order forces and contact mechanics must be taken into account. Such

issues have been examined before in the context of single robots or small groups of two to three robots [12], [18], [24], [22]. Behavior based approaches yield interesting results but lack performance guarantees [20], [15], [8], [11].

Marine applications with a high number of actuators have been considered before as well, but exclusively in the context of large vessels with "thruster pods" such as commercial cruise ships [6], [9], [17] and [27]. As such, in each of these works, the control scheme is completely centralized with no uncertainty in the location or actions of the actuators.

Closely related works on distributed swarm manipulation are [23], [26], and [16]. Within these works, controllers were designed to force robots to surround the object. Inter-robot spacing was constrained to be small enough that it is impossible for the object to "escape" – meaning that as the robots move, so must the object. While this approach is decentralized, the primary drawback is that it was designed for land-based robots. Therefore, they treat the task as a position control problem and ignoring the dynamic forces, momentum and actuator saturation.

In this paper we present a control strategy that enables the barge to track a reference trajectory. It accounts for second order dynamics, actuator limitations, and model uncertainty associated with linear drag effects. A special property of the controller, when used in conjunction with the force allocation strategy presented here and grasp synthesis approach in companion work, is that it is asymptotically stable despite actuator limitations on individual swarm members. In the authors' previous work [2], a commutation strategy was employed to exactly distribute the force/torque command among the swarm members; however, the tugboats must be aligned in a precise opposing pair configuration along the barge hull. Though this approach offers a method by which to guarantee that the swarm's combined effort produces the commanded request; maintaining the exact alignment may be difficult in heavy sea states. Therefore in this work, we wish to investigate the possibility of utilizing an alternative optimization approach for force/torque

allocation. In addition, in-water experiments show that it is also able to compensate for model uncertainties associated with drag coefficient uncertainties, which is a critical issue for practical implementation in the marine setting.

The remainder of the paper is organized as follows. In Section II, we provide the second order dynamic model of the marine vessel and formalize the problem statement. In Section III, we present the high level tracking, adaptive controller along with our force allocation methodology in Section IV. In Section V, simulation results are provided, and the experimental test bed and results are presented in Sect. VI. Section VII summarizes our contributions and discusses our future work.

II. System Model

We refer to the object to be manipulated, as a barge. Mathematically, it is defined by a compact, convex set $\mathcal{O} \subset \mathbb{R}^2$. Define a body-fixed coordinate frame $(\hat{i}, \hat{j})$ attached to the centroid of $\mathcal{O}$ (see Figure 1). Ignoring heave (vertical), pitch and roll motions, a planar 3 DOF model, low speed model is [6]

$$\dot{P} = R(\psi)\nu \qquad (1)$$
$$M\dot{\nu} + D\nu = u_{net} \qquad (2)$$

where $P = [x, y, \psi]^T$ denotes the inertial (x, y) position and barge heading (ψ), $\nu = [v_x, v_y, \omega]^T$ is the barge's velocity expressed in the body frame (also called surge, sway and yaw rate). $R(\psi)$ denotes the rotation matrix from the body frame to the inertial frame and is defined as follows

$$R(\psi) = \begin{bmatrix} \cos(\psi) & -\sin(\psi) & 0 \\ \sin(\psi) & \cos(\psi) & 0 \\ 0 & 0 & 1 \end{bmatrix}. \qquad (3)$$

$M = \text{diag}\{m_x, m_y, I_z\} \in \mathbb{R}^{3 \times 3}$ represents the mass/inertia matrix that includes added mass [6], and $D = \text{diag}\{X_u, Y_v, N_r\} \in \mathbb{R}^{3 \times 3}$ represents the hydrodynamic drag matrix (for our low speed application, only linear drag is considered).

The right hand side of (2) is the net applied wrench on the barge, $u_{net} = [F_x, F_y, M_z]^T$ due to the N tugboats. Note that in practice, actual tugboats:

1) "tie-up" to the barge, meaning that their configuration is nominally time invariant and their ability to transfer forces is not friction dependant;
2) have propellers and engines that are significantly less efficient when run in reverse; and
3) have upper limits on the thrust they can apply – very often two or more tugs are required to generate enough force to move the barge.

Reflecting these assumptions, $u_{net} = Bu$, where $u = [u_1, \ldots u_N]^T \in U$ is a vector of input push force magnitudes for each tugboat. The set U is described as $0 \leq u_i \leq u_{\max}, \forall i \in [1, N]$. $B \in \mathbb{R}^{3 \times N}$ captures the geometric configuration of the tugs and requires additional notation.
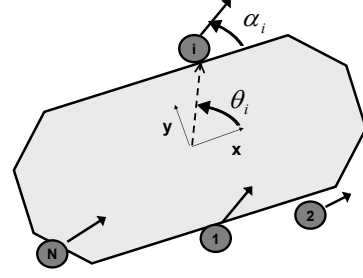
Fig. 1. Swarm Manipulation Scenario. N robots(dark circles) are attached to the object (shaded polygon); and can apply forces at some fixed incident angles. The position of the ith boat is determined by angle θ_i and the push direction by the angle α_i.

The barge boundary is denoted by $\partial\mathcal{O}$, assuming it is convex allows us to parameterize the points on the boundary using the angle θ, measured counter clockwise, relative to the x axis of the body frame:

$$\{x(\theta)\hat{i} + y(\theta)\hat{j} \in \partial\mathcal{O}, \forall \theta \in \mathbb{S}^1\} \qquad (4)$$

in addition, define a parameter $\alpha \in \mathbb{S}^1$ which indicates the direction of the push force, measured counter clockwise relative to the $\hat{i}$-axis of the body frame. Then the contact configuration of the ith robot can be described by a vector $[\theta_i, \alpha_i]^T$. The ith column is

$$B_i = \begin{bmatrix} \cos(\alpha_i) \\ \sin(\alpha_i) \\ -y(\theta_i)\cos\alpha_i + x(\theta_i)\sin\alpha_i \end{bmatrix}. \qquad (5)$$

Note that there is no constraint on the allowed push directions, α_i, as there would be in the case of friction assisted grasping. Throughout this paper we assume that the configuration of the tugboats (and hence the B matrix) represents a force closure grasp. Force closure is defined as the ability of a robot grasp to resist or apply a wrench in an arbitrary direction. Due to the unilateral constraint that the tugboat forces u are nonnegative, in order to achieve force closure the set of possible applied wrenches at all the contacts (i.e. the columns of B) must positively span $\mathbb{R}^3$; this condition is easily tested [13]. For this application stating that the grasp is a force closure configuration, is equivalent to saying that the position and orientation of the object is small time locally controllable, under the constraint that the applied forces are nonnegative. It is a well known result that at least 4 contacts [13] are required to satisfy this condition for the class of objects and contact types considered here. Therefore, in this paper we assume that the swarm size $N \geq 4$. Note that, given the B matrix it is possible to compute an upper bound on u_{net} consistent with the constraints on u

$$\bar{u}_{net} = \min_{jk \in N \times N} u_{\max} \sum_{i=1}^{N} \max(0, \frac{B_j \times B_k}{\|B_j \times B_k\|} \cdot B_i). \qquad (6)$$

Synthesizing the optimal placement of the tugs is beyond the scope of this paper, but is addressed in other work from our group [3].

III. Tracking Control Design

Problem 3.1: Given, the nominal ship model from (1), a reference trajectory $P_d(t)$, measurements of P and $\dot{P}$, and the upper bound on the thrust the swarm can generate in all directions $\bar{u}_{net}$; determine a feedback law $U : \mathbb{R}^6 \to u_{net}$ such that $\|u_{net}(t)\| \le \bar{u}_{net}, \forall t \in \mathbb{R}^+$.

In order to promote this position objective, the following error signals are defined

$$e_p = R^T(\psi)(P_d - P), \quad e_\nu = \nu - R^T(\psi)\dot{P}_d \qquad (7)$$

where $P_d(t) \in \mathbb{R}^3$ represents a sufficiently smooth (i.e., differentiable) position/orientation trajectory. In order to facilitate the design of the 2nd order system, the filter tracking error $r(t) \in \mathbb{R}^3$ is specified as follows

$$r(t) = e_\nu + k_p e_p \qquad (8)$$

where $k_p \in \mathbb{R}^+$ denotes a positive, scalar control gain. In order to account for unknown hydrodynamic drag parameters, the following parameter estimation error signal $\tilde{\Theta}(t) \in \mathbb{R}^3$ is defined in the following manner

$$\tilde{\Theta} = \Theta - \hat{\Theta} \qquad (9)$$

where $\hat{\Theta}(t) = \left[\hat{X}_u, \ \hat{Y}_v, \ \hat{N}_r\right]^T \in \mathbb{R}^3$ denotes the yet to be designed parameter estimate vector. In order to proceed with the design of the tracking controller, we first develop the open-loop position/velocity tracking systems [19]

$$\begin{aligned} \dot{e}_p &= -S(\nu)e_p + e_\nu \\ \dot{e}_\nu &= \dot{\nu} + S(\nu)R^T(\psi)\dot{P}_d - R^T(\psi)\ddot{P}_d \end{aligned} \qquad (10)$$

where the skew-symmetric matrix $S(\nu)$ is given as

$$S(\nu) = \begin{bmatrix} 0 & -\omega & 0 \\ \omega & 0 & 0 \\ 0 & 0 & 0 \end{bmatrix}. \qquad (11)$$

In order to design the control input u_{net}, the open-loop filtered tracking error dynamics are developed in the following manner

$$\begin{aligned} M\dot{r} &= [-Y(\nu)\Theta + u_{net}] + M\left[S(\nu)\left(R^T(\psi)\dot{P}_d - k_p e_p\right)\right. \\ &\quad \left. - R^T(\psi)\ddot{P}_d + k_p e_\nu\right] \end{aligned} \qquad (12)$$

where the regression matrix $Y(\nu)$ and the unknown parameter vector Θ are defined by the following expressions

$$Y(\nu) = \begin{bmatrix} u & 0 & 0 \\ 0 & v & 0 \\ 0 & 0 & \omega \end{bmatrix}, \Theta = \begin{bmatrix} X_u \\ Y_v \\ N_r \end{bmatrix}. \qquad (13)$$

Based on the open-loop tracking error dynamics, the vessel control input $u_{net}(t)$ to promote position tracking is specified in the following manner

$$\begin{aligned} u_{net} &= Y(\nu)\hat{\Theta} - M\left[S(\nu)\left(R^T(\psi)\dot{P}_d - k_p e_p\right)\right. \\ &\quad \left. - R^T(\psi)\ddot{P}_d + k_p e_\nu\right] - e_p - k_r r \end{aligned} \qquad (14)$$

where $k_r \in \mathbb{R}^+$ denotes a positive, scalar control gain (note that k_r could be defined as a positive definite, diagonal gain matrix).In order to calculate a suitable upper bound on the required forces/torque of (14), the following projection based update law is employed to generate a bounded parameter estimate vector $\hat{\Theta}(t)$

$$\dot{\hat{\Theta}} = \begin{cases} 0 & \text{if } \hat{\Theta} = \bar{\Theta}, -Y^T(\nu)r > 0 \\ 0 & \text{if } \hat{\Theta} = 0, -Y^T(\nu)r < 0 \\ -Y^T(\nu)r & \text{otherwise} \end{cases} \qquad (15)$$

where $\bar{\Theta}$ denotes the upperbound values for the drag coefficients (assumed known). After substituting in the control force/torque vector $u_{net}(t)$ into the open-loop dynamics of (12), the following closed-loop dynamics are obtained for $r(t)$

$$M\dot{r} = -Y(\nu)\tilde{\Theta} - e_p - k_r r \qquad (16)$$

Stability and the position tracking result can be illustrated through Lyapunov analysis by defining the following non-negative scalar function $V(t)$ as

$$V = \tfrac{1}{2}e_p^T e_p + \tfrac{1}{2}\tilde{\Theta}^T\tilde{\Theta} + \tfrac{1}{2}r^T M r \qquad (17)$$

After taking the time derivative of (17) and substituting in the expressions of (10), (15), and (16), the time derivative for $V(t)$ can be upperbounded by the following expression

$$\dot{V} \le -\alpha\|e_p\|^2 - k_r\|r\|^2 \qquad (18)$$

where the fact that $e_\nu = r - \alpha e_p$ has been utilized. Barbalat's Lemma [10] can now be applied to (18) to illustrate asymptotic position tracking in the sense that $\lim_{t \to \infty} e_p(t), r(t) = 0$.

Remark 3.2: In an effort to promote a more fieldable solution, one of the objectives of this work was to consider actuator constraints. In the above tracking controller, the commanded force/torque vector $u_{net}(t)$ is not directly saturated as was done in [5]. Rather, the asymptotic stability result coupled with an appropriate desired trajectory generator can offer some ability to influence the limits on $u_{net}(t)$. Since $\dot{V}(t) \le 0$ from (18), then it is known that after some time the error signals may be neglected from the $u_{net}(t)$ leaving the following terms

$$u_{net} \approx Y(R^T\dot{P}_d)\Theta + MS(R^T\dot{P}_d)R^T\dot{P}_d - MR^T\ddot{P}_d \quad (19)$$

where we have utilized the assumption that enough time has elapsed such that $\nu \to R^T(\psi_d)\dot{P}_d$. From the expansion of (19), the following bounding expression can be obtained

$$|u_{net}| \le \begin{bmatrix} \left(X_{\bar{u}} + m_x|\dot{\psi}_d|\right)(|\dot{x}_d| + |\dot{y}_d|) + m_x(|\ddot{x}_d| + |\ddot{y}_d|) \\ \left(Y_{\bar{v}} + m_y|\dot{\psi}_d|\right)(|\dot{x}_d| + |\dot{y}_d|) + m_y(|\ddot{x}_d| + |\ddot{y}_d|) \\ N_{\bar{r}}|\dot{\psi}_d| + I_z|\ddot{\psi}_d| \end{bmatrix}$$

From the structure of the above expression, the selection of the desired velocity/accelerations can be done in

such a manner as to ensure that the command vector $u_{net}(t)$ does not exceed the cooperative capabilities of the swarm.

IV. Thrust Allocation Strategy

With the design of $u_{net}(t)$, the subsequent task is to now specify the individual tugboat thrusts such that their combined effort generates as closely as possible $u_{net}(t)$. Therefore, the thrust allocation strategy must solve the following linearly constrained least squares problem.

Problem 4.1: Given a u_{net} from (1), determine $u \in \mathbb{R}^N$ according to

$$\min_u \|Bu - u_{net}\|^2 \tag{20}$$

such that

$$0 \leq u_i \leq u_{\max}, \quad i = 1, \ldots, N. \tag{21}$$

Remark 4.2: The linearly constrained least squares problem is known to be convex, therefore it returns a globally optimal solution. Furthermore, its solution is efficient enough to be computed in real time as part of the feedback law and scales well, $O(N^2)$, with swarm size [1].

V. Simulation Results

The primary focus of the simulation studies is to investigate the performance of the optimization approach of Section IV for force/torque allocation. To this end, a barge having the following mass and drag values [17] was simulated within the MATLAB SIMULINK environment

$$M = \text{diag}\{ \ 19.0 \ (kg), \quad 35.2 \ (kg), \quad 4.2 \ (kg \cdot m^2) \ \}$$
$$D = \text{diag}\{ \ 4.0 \ (\tfrac{N \sec}{m}), \quad 10.0 \ (\tfrac{N \sec}{m}), \quad 1.0 \ (Nm \cdot \sec) \ \} \tag{22}$$

The swarm configuration about the barge hull was selected according to [19] as follows

$$
\begin{aligned}
&\alpha_1 = 180°, \quad r_1 = 0.60 \ (m), \quad \theta_1 = 0° \\
&\alpha_2 = 270°, \quad r_2 = 0.27 \ (m), \quad \theta_2 = 45° \\
&\alpha_3 = 270°, \quad r_3 = 0.19 \ (m), \quad \theta_3 = 90° \\
&\alpha_4 = 0°, \qquad r_4 = r_1, \qquad\quad \theta_4 = 180° \\
&\alpha_5 = 90°, \quad\; r_5 = r_2, \qquad\quad \theta_5 = 315° \\
&\alpha_6 = 90°, \quad\; r_6 = r_3, \qquad\quad \theta_6 = 270°
\end{aligned}
\tag{23}
$$

Remark 5.1: Note that the placement in (23) reflects the placement of thrusters about the USNA yard patrol experimental platform (see Figure 4) yet the barge dynamics reflect the vessel of [17]. This mistmatch was allowed since accurate drag coefficients have not been established for the USNA vessel.

In an effort to limit actuator requirements, the following trapezoidal velocity desired trajectory [21] was employed for point to point movements/rotations

$$
x_d \;=\;
\begin{cases}
x_0 + \frac{\alpha_x}{2}t^2 & 0 \leq t \leq t_b \\[2mm]
\frac{x_f + x_0 - V_x t_f}{2} + V_x t & t_b < t \leq (t_f - t_b) \\[2mm]
x_f - \frac{\alpha_x t_f^2}{2} + \alpha_x t_f t - \frac{\alpha}{2}t^2 & (t_f - t_b) < t \leq t_f
\end{cases}
$$
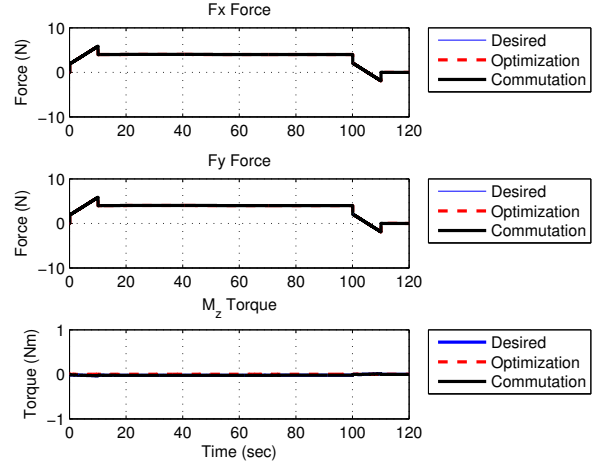
Fig. 2.   Simulated Forces/Torques

where α_x and V_x represent the desired barge acceleration and velocity, respectively. The blending time t_b and the arrival time t_f can be calculated according to [21]. The desired position and rotation trajectories for $y_d(t)$ and $\psi_d(t)$ are specified in an analogous manner. For the subsequent simulation, the acceleration and velocity coefficients were selected as

$$
\begin{aligned}
&\alpha_x = \alpha_y = 0.1 \ \left(\tfrac{m}{\sec^2}\right), \quad \alpha_\psi = 0.0175 \ \left(\tfrac{rad}{\sec^2}\right) \\
&V_x = V_y = 1.0 \ \left(\tfrac{m}{\sec}\right), \qquad V_\psi = 0.1 \ \left(\tfrac{rad}{\sec}\right) \\
&x_f, y_f = 100.0 \ (m), \qquad \psi_f = 0.0 \ (rad)
\end{aligned}
\tag{24}
$$

For the command vector u_{net} of (14) and the force allocation method of (20), the following control gains and maximum thruster output were specified as

$$\alpha = 10.0, \quad k_r = 2.0, \quad u_{\max} = 50.0 \ (N). \tag{25}$$

Figure 2 illustrates the developed forces/torques of the swarm configuration from the optimization allocation method of (20).

VI. Experimental Results

In order to offer experimental validation of the control strategies presented in the previous sections, a small scale experimental vessel was built (see Figure 4). The hull of the "barge" is a $1/36^{th}$ scale model of a U.S. Navy Yard Patrol craft. It measures approximately 1.0 m in length and 0.3 m wide. Six marine bilge pumps were attached to the vessel to act as our swarm of tug boats. Each bilge pump is powered by a 12.0 V, H-bridge power amplifier, the mechanical design of the pumps is such that they can only produce thrust in one direction. The maximum value of the thrust is approximately 5 (N).

The control strategy is executed using the on-board Rabbit 3000 microprocessor. Since the setup is intended to be utilized inside USNA's 100.0 meter tow tank facility, standard global positioning sensors could not be employed to provide the inertial position and heading
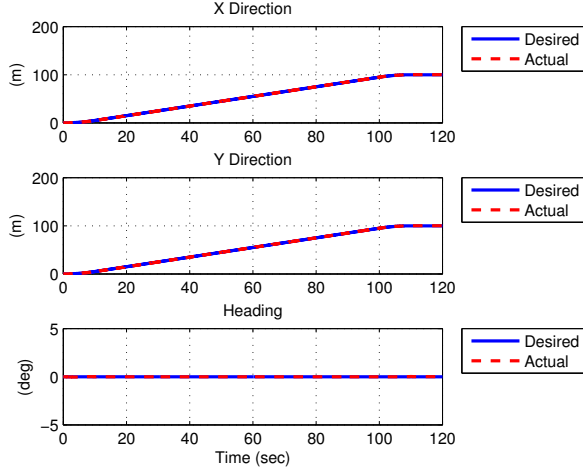
Fig. 3. (a) (x, y) Position of Barge COM, (b) Heading ψ of Barge
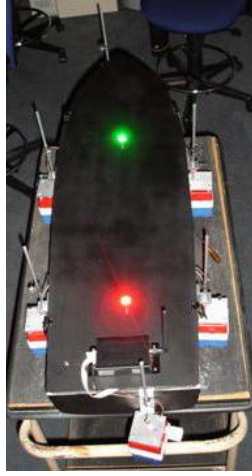
Fig. 4. USNA Experimental Swarm Vessel

signals. Instead, a standard web camera was mounted overhead the workspace and interfaced with MATLAB's Image Acquisition Toolbox. Two high intensity LEDs mounted on top of the vehicle provide active color features from which the x, y position and heading of the vessel in the image plane is determined. The camera provides a 640×480 pixel image, and with the camera being mounted approximately 8.0 meters overhead, a resolution of approximately 0.02 $m/pixel$ is obtained. The position/orientation measurements were transmitted to the ship-board Rabbit processor via pair of MaxStream Wireless RS232 serial modems. The required velocity signals of $\dot{P}(t)$ were generated through a backwards difference scheme coupled with a low pass filter. The numerical values for the mass matrix of the USNA vessel differs slightly than that of [17] and are approximated as

$$M = \text{diag}\{ \ 15.5 \ (kg), \quad 15.5 \ (kg), \quad 1.5 \ (kg \cdot m^2) \ \}$$
(26)
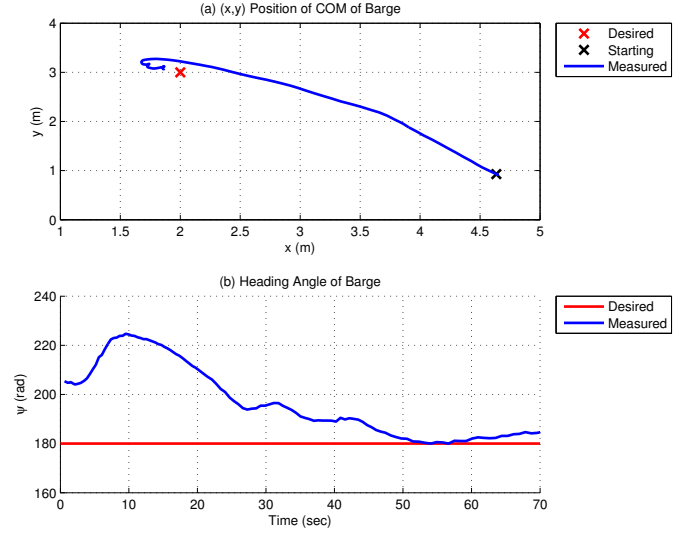
Fig. 5. (a) (x, y) Barge COM Position (b) Heading ψ of Barge.

Since exact drag coefficients are not available for this vessel, this offers a perfect scenario under which to evaluate the adaptive controller's ability to compensate for unknown drag effects.

Remark 6.1: For the experimental results, we would like to point out that the commutation strategy of [2] was utilized to allocate forces/torques among the swarm tugs in lieu of the optimization strategy of (20). In addition, the experimental controller operated as a regulating controller meaning that $\dot{P}_d(t) = \ddot{P}_d(t) = 0$).

For the experiment, the barge was located at the following initial position/orientation with the desired position/orientation is selected as

$$
\begin{aligned}
P(0) &= \begin{bmatrix} 4.64 \ (m), & 0.93 \ (m), & 205.40^o \end{bmatrix}^T \\
P_d(t) &= \begin{bmatrix} 2.0 \ (m), & 3.0 \ (m), & 180.0^o \end{bmatrix}^T
\end{aligned}
$$
(27)

The control gains were selected as follows

$$\alpha = 0.3, \quad k_r = 0.5,$$
(28)

and the initial values for the parameter estimate vector $\Theta(t)$ was selected as

$$\Theta(0) = \begin{bmatrix} 0.05, & 1.5, & 0.15 \end{bmatrix}^T$$
(29)

The (x, y) position of the center of mass of the barge and the barge heading angle ψ is illustrated in Figure 5 with the parameter estimates for the drag effects are shown in Figure 6.

Remark 6.2: It should be noted that the adaptive update law of (15) was not designed for identification of the drag coefficients $D = \text{diag}\{X_u, Y_v, N_r\}$; rather, the dynamic equation of (15) was specified in an effort to promote the position/orientation tracking error objective by ensuring that the Lyapunov function $V(t)$ is negative semi-definite. From Figure 6, one can observe that the parameter estimates approach to a constant value
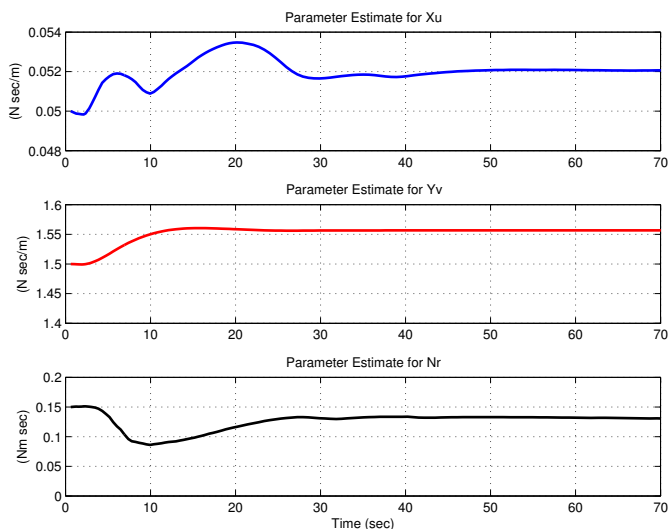
Fig. 6.   Parameter Estimates for Drag Effects

in approximately 40.0 (sec) which coincides with the approach of the disabled vessel to its desired coordinates.

VII. Conclusions

In this paper, two major investigations were performed. First, an optimization based force/torque allocation was employed and compared against a commutation based force/torque allocation strategy. This optimization allocation strategy is of interest due to the commutation approach being susceptible to failure in heavy sea states. In addition, experimental results illustrating the ability of the adaptive compensation of hydrodynamic effects on a small scale experimental test stand have been illustrated. Future work will focus on the inclusion of force/torque mismatch between the high level control u_{net} and that developed by the collective swarm Bu within the stability analysis. Furthermore, open-water experimental verification on the adjacent Severn River is planned.

Acknowledgments

References

[1] S. Boyd and L. Vandenberghe. Convex Optimization. Cambridge University Press, 2004.

[2] D. Braganza, M. Feemster, and D. Dawson. Positioning of large surface vessles using multiple tugboats. In IEEE American Control Conference, pages 912–917, 2007.

[3] J.M. Esposito. Distributed grasp synthesis for swarm manipulation. Submitted to ICRA 2008.

[4] J.M. Esposito and T.W. Dunbar. Maintaining wireless connectivity constraints for swarms in the presence of obstacles. In IEEE Conference on Robotics and Automation, pages 946–952, 2006.

[5] M. Feemster, Y. Fang, and D. Dawson. Disturbance rejection for a magnetic levitation systsm. In IEEE Transactions on Mechatronics, pages 709–717, 2006.

[6] Thor I. Fossen. Marine Control Systems. Marine Cybernetics, Norway, 2002.

[7] V. Gazi and K.M. Passiano. Stability analysis of swarms. IEEE Transactions on Automatic Control, 48(4):692–696, 2003.

[8] A.J. Ijspeert, A. Martinoli, A. Billard, and L.M. Gambardella. Collaboration through the exploitation of local interactions in autonomous collective robotics: The stick pulling experiment. Autonomous Robots, 11(2):149171.

[9] T. Johansen, T. Fossen, and S. Berge. Constrained nonlinear control allocation with singularity avoidance using sequential quadratic programming. IEEE Transactions On Control Systems Technology, pages 211–216, 2004.

[10] Hassan K. Khalil. Nonlinear Systems. Prentice Hall, New Jersey, 2001.

[11] R. Kube and E. Bonabeau. Cooperative transport by ants and robots. Robotics and Autonomous Systems, 30(1-2):85–101, 2000.

[12] K.M. Lynch. Locally controllable manipulation by stable pushing. IEEE Transactions on Robotics and Automation, pages 318–327, 1999.

[13] R. Murray, Z. Li, and S. Sastry. A Mathematical Introduction to Robotic Manipulation. CRC Press, 1994.

[14] R. Olfati-Saber and R. Murray. Flocking with obstacle avoidance: cooperation with limited communication in mobile networks. In IEEE Conference on Decision and Control, 2003.

[15] C.A. Parker, H. Zhang, and R. Kube. Blind bulldozing: Multiple robot nest construction. In IEEE/RSJ International Conference on Intelligent Robots and Systems, pages 2010–2015.

[16] G. Pereira, V. Kumar, and M. Campos. Decentralized algorithms for multi-robot manipulation via caging. International Journal of Robotics Research, 2004.

[17] K.Y. Pettersen, F. Mazenc, and H. Nijmeiejer. Global uniform asymptotic stabilization of an underactuated surface vessle: Experimental results. IEEE Transactions on Control Systems Technology, 12(6):891–903, 2004.

[18] D. Rus. Coordinated manipulation of objects in the plane. Algorithmica, pages 129–147, 1997.

[19] E. Smith, M. Feemster, J. Esposito, and J. Nicholson. Swarm manipulation an unactuated surface vessel. In IEEE Southeastern Symposium on Systems Theory, pages 16–20, 2007.

[20] P. Song and V. Kumar. A potential field based approach to multi-robot manipulation. In IEEE International Conference on Robotics and Automation, pages 1217–1222, 2002.

[21] M. Spong, S. Hutchinson, and M. Vidyasagar. Robot Modeling and Control. John Wiley and Sons, New York, 2006.

[22] D.J. Stilwell and J.S. Bay. Optimal control for cooperating mobile robots bearinga common load. In IEEE International Conference on Robotics and Automation, pages 58–63, 1994.

[23] A. Sudsang and J. Ponce. A new approach to motion planning for disc shaped objects in the plane. In IEEE Conference on Robotics and Automation, pages 1068–1075.

[24] T. Sugar and V. Kumar. Control of cooperating mobile manipulators. IEEE Transactions on Robotics and Automation, 18(1):94 – 103, 2002.

[25] H.G. Tanner, A. Jadbabaie, and G.J. Pappas. Stable flocking of mobile agents, part I: fixed topology. In IEEE Conference on Decision and Control, 2003.

[26] Z.D. Wang, E. Nakano, and T. Takahashi. Solving function distribution and behavior design problem for cooperative object handling by multiple mobile robots. IEEE Transactions on Systems, Man, and Cybernetics, Part A, 33(5):537–549, 2003.

[27] W. C. Webster and J. Sousa. Optimum allocation for multiple thrusters. In Proc. Int. Soc. Offshore and Polar Engineers Conf, 1999.